PHYSICAL REVIEW E **68**, 045102(R) (2003)

Coupling-induced oscillations in overdamped bistable systems

Visarath In,[1,*] Adi R. Bulsara,[1,†] Antonio Palacios,[2,‡] Patrick Longhini,[2] Andy Kho,[1] and Joseph D. Neff[1]
[1]*Space and Naval Warfare Systems Center, Code 2363, 53560 Hull Street, San Diego, California 92152-5001, USA*
[2] *Nonlinear Dynamics Group, Department of Mathematics & Statistics, San Diego State University, San Diego, California 92182, USA*
(Received 24 July 2003; published 14 October 2003)

It is well known that overdamped and unforced dynamical systems do not oscillate. However, well-designed coupling schemes, together with the appropriate choice of initial conditions, can induce oscillations when a control parameter exceeds a threshold value. We demonstrate this effect in a specific system, a soft-potential mean-field description of the dynamics in a (hysteretic) single-domain ferromagnetic sample. Using a specific (unidirectional, with cyclic boundary conditions) coupling scheme, together with nonidentical initial conditions, one can cause the coupled system of N elements (N odd) to oscillate when the coupling coefficient is swept through a critical value. The ensuing oscillations could find utility in the detection of very weak ''target'' signals, via their effect on the oscillation characteristics.

DOI: 10.1103/PhysRevE.68.045102 PACS number(s): 02.50.Ey, 05.10.Gg, 05.40.−a, 85.70.Ay

Overdamped bistable dynamics, of the generic form $\dot{x} = -\nabla U(x)$, underpin the behavior of numerous systems in the physical world. The most-studied example is the overdamped Duffing system, the dynamics of a particle in a bistable potential $U(x) = -ax^2 + bx^4$. Without an external forcing term, the state point $x(t)$ will rapidly relax to one of two stable attractors, for any choice of the initial condition. It has been shown [1], however, that coupling similar elements via a linear unidirectional coupling with cyclic boundary conditions can lead to oscillatory behavior past a critical value of the coupling coefficient. Typically, this behavior is dictated by symmetry conditions [2], and is generated via Hopf bifurcations; it appears to occur in any coupled system of overdamped bistable elements, none of which would oscillate when isolated and undriven, subject to the appropriate choice of parameters and operating conditions (albeit through different bifurcation mechanisms). Here, we focus on a specific system in which the state point $x(t)$ represents the (suitably normalized) magnetic induction in a ferromagnetic sample. The dynamical model is obtained via the continuum limit of a discrete spin model of individual domain dynamics [3], and has been recently used [4] to characterize the response of a specific magnetic measurement system, the fluxgate magnetometer:

$$\dot{x} = -x + \tanh[c(x+\epsilon)], \tag{1}$$

where the overdot denotes the time derivative and c denotes a temperature- and material-dependent system parameter governing bistability (the system is bistable for $c>1$). ϵ is an (typically much smaller than the energy barrier height, and taken to be dc throughout this work) external target signal that one wishes to detect; its effect is to render the potential $U(x)$ asymmetric, and detection techniques are aimed at quantifying this asymmetry. Traditional magnetic detection using this device (see Ref. [4] for an overview and references) can be constrained by cumbersome electronics and large on-board power requirements. Recent innovations [4] have lead to a readout scheme based on the crossing times statistics in the presence of a noise floor, and our studies [4,5] indicate that lowering the bias signal amplitude and frequency can enhance sensitivity and resolution, although practical constraints may limit the extent of such a reduction. In any case, this recent work [4] has suggested a new generation of inexpensive, low-power, and more-noise-tolerant sensors, having dynamics qualitatively similar to the ferromagnetic core based magnetic sensor modeled by Eq. (1). The coupling scheme and resulting oscillatory behavior that we discuss below, therefore, afford the possibility of even greater power savings and ease of operation of a large class of devices/systems, underpinned by overdamped bistable dynamics; in essence, the immediate practical benefit would be the ability to operate these sensors with significantly lower power.

For clarity and ease of calculation, we return to the basic dynamics (1) for three identical coupled elements:

$$\begin{aligned}
\dot{x}_1 &= -x_1 + \tanh[c(x_1 + \lambda x_2 + \epsilon)], \\
\dot{x}_2 &= -x_2 + \tanh[c(x_2 + \lambda x_3 + \epsilon)], \\
\dot{x}_3 &= -x_3 + \tanh[c(x_3 + \lambda x_1 + \epsilon)].
\end{aligned} \tag{2}$$

Notice that the (unidirectional) coupling term, having strength λ, which is assumed to be equal for all three elements, is *inside* the nonlinearity, a direct result of the mean-field nature of the description (in the fluxgate magnetometer, the coupling is through the induction in the primary or ''pick up'' coil).

A simple numerical integration of Eq. (2) (starting with *nonidentical* initial conditions) reveals oscillatory behavior for $\lambda < \lambda_c$, where λ_c is a critical threshold value of coupling strength [it will become apparent, later, that $\lambda_c < 0$ in the convention adopted in Eq. (2)]. The oscillations are nonsinusoidal, with a frequency that increases as the coupling

*Electronic address: visarath.in@navy.mil
†Electronic address: adi.bulsara@navy.mil
‡Electronic address: palacios@euler.sdsu.edu

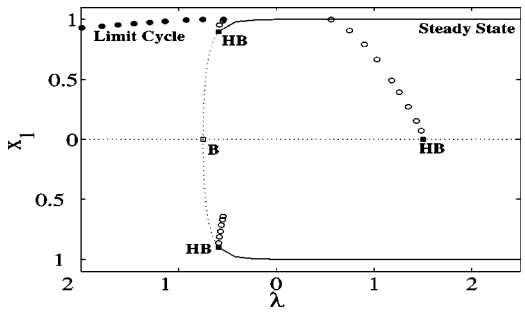

FIG. 1. Bifurcation diagram for a system of three identical elements (2) coupled in a directed ring. Filled squares represent local Hopf bifurcations of unstable periodic solutions (empty circles); empty square describes a steady-state pitchfork bifurcation point of two branches of nontrivial unstable equilibria (dotted lines). Filled circles represent stable periodic solutions created via global bifurcations. $c=3$, $\epsilon=0$.

strength decreases away from λ_c. For $\lambda>\lambda_c$, however, the system quickly settles into a steady state that depends on the initial conditions.

A detailed bifurcation analysis of the oscillatory behavior in response to parameter changes must start with the fundamental question about its origin. To aid the analysis, the software package AUTO [6] and the theory of Hopf bifurcation with symmetry [2] are employed. We first write the coupled system in a more compact form $\dot{x}_i=f(x_i,x_{i+1},\lambda,\epsilon)$, $i=1,2,\ldots,N$.

Then under the unidirectional coupling scheme, the *global* symmetries of this system with $N=3$ are described by the cyclic group $\mathbf{Z}_3$, generated by the permutation $(x_1,x_2,x_3)\mapsto(x_3,x_2,x_1)$. By ''global'' symmetries we mean the symmetries that are induced by the pattern of coupling [7]. In contrast, *local* symmetries refer to symmetries of each individual element; these symmetries are described by the group $\mathbf{Z}_2$, generated by $x\mapsto -x$. We first fix $\epsilon=0$, $c=3$, and vary λ, so that $(x_1,x_2,x_3)=(0,0,0)$ is a Z_3 symmetric trivial equilibrium. Linearizing at the origin, yields the Jacobian

$$J=(df)_{(\lambda,c=3,\epsilon=0)}=\begin{bmatrix} 2 & 3\lambda & 0 \\ 0 & 2 & 3\lambda \\ 3\lambda & 0 & 2 \end{bmatrix},$$

whose eigenvalues $\beta_1=2+3\lambda$, $\beta_{2,3}=2-\frac{3}{2}\lambda\pm 3\sqrt{3}/2\lambda i$ suggest two primary local bifurcation points off the origin: a Hopf bifurcation (HB) at $\lambda=4/3$ and a steady-state bifurcation (B) at $\lambda=-2/3$. In fact, AUTO reveals (see Fig. 1) that one branch of unstable periodic solutions (open circles) bifurcates off the origin at $\lambda=4/3$, and two branches of unstable nontrivial equilibrium points (dotted lines) emerge at $\lambda=-2/3$ via a pitchfork bifurcation. Both branches of nontrivial equilibria simultaneously become stable, at $\lambda=-0.5018$, when two additional branches of unstable periodic solutions emerge via secondary Hopf bifurcations off each nontrivial equilibrium branch. As λ increases past these secondary HB points, the equilibrium branches asymptotically approach ± 1; and the typical behavior of the system is to settle into a steady state. Which steady state is actually observed depends on the initial condition of each element. On the other hand, when $\lambda<\lambda_c$, a branch of stable limit cycles (filled circles) appears. Numerically, the critical point is found to be $\lambda_c=-0.4345$ for the case of $\epsilon=0$ and $c=3$. For $\lambda\ll\lambda_c$, the limit cycle has amplitude $O(1)$, and as $\lambda\to-\infty$, the oscillations approach a constant amplitude value, ≈ 0.5. The limit cycle is globally stable; its basin of attraction spans almost the entire phase space. Even a slight variation in the initial condition, away from $x_1=x_2=x_3$, will push the system into the oscillatory solution. This is particularly significant for practical purposes, wherein operational constraints (e.g., a noise floor) would make it near impossible to have identical $x_i(0)$. As λ increases (starting from a large negative value) towards λ_c, the amplitude of the limit cycle remains around unity, decreasing abruptly to zero at the critical point; the frequency also decreases towards zero. Thus the limit cycle oscillations are ''full grown'' everywhere they exist, which suggests that a global bifurcation is responsible for their creation and annihilation. Figure 2 provides a phase-space depiction of the growth of the limit cycle oscillations as λ varies.

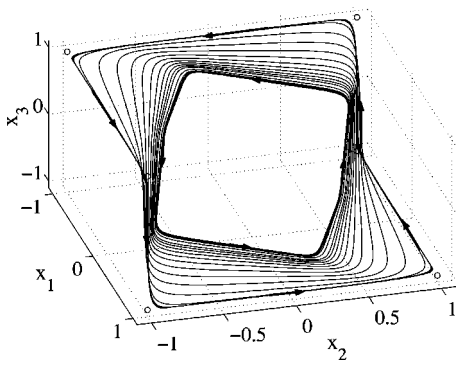

FIG. 2. Stable limit cycle solutions with amplitude $O(1)$ appear in system (2) for large negative values of λ. Fixed parameters are $c=3$, $\epsilon=0$. The arrows indicate the direction of the flow.

We now investigate the global bifurcation that leads to stable periodic oscillations, and seek an analytic expression for the critical point λ_c. It is well known that a generic feature of symmetric nonlinear systems is the existence of *heteroclinic cycles*, defined as a collection of solution trajectories that connect sequences of equilibria and/or periodic solutions [8]. Heteroclinic cycles are highly degenerate. Certain symmetries, however, can facilitate the existence of cyclic trajectories that can ''travel'' through invariant subspaces while connecting, via saddle-sink connections, one solution to another. In Eq. (2), in particular, we find six near-invariant planar regions (with $\lambda<0$):

$$\delta_i=\{x_i:\lambda x_i<1,\ \ x_{(i+2 \bmod 3)}=-1\},\quad i=1,2,3,$$

$$\delta_i=\{x_i:\lambda x_i>-1,\quad x_{(i+2 \bmod 3)}=1\},\quad i=4,5,6.$$

Then the solution trajectories on the cycle lie on flow-invariant lines (see Fig. 2) defined by the intersection of the invariant planes. A typical trajectory on the cycle connects six saddle points located near the points $(1,-1,-1)$, $(1,1,-1)$, $(-1,1,-1)$, $(-1,1,1)$, $(-1,-1,1)$, and $(1,-1,1)$.

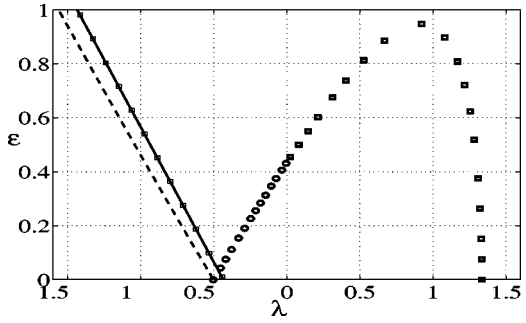

FIG. 3. Two-parameter continuation of Hopf bifurcation points (dashed line, empty circles, and squares) and heteroclinic connections (black line obtained numerically via AUTO, superimposed squares obtained analytically). Periodic solutions are globally stable only for parameter values (λ,ϵ) below the black line, and unstable everywhere else. $c=3$.

The saddle points exist only for $\lambda>\lambda_c$ and are annihilated when the periodic solutions appear. This suggests that we could determine the exact location of the heteroclinic cycle by finding the regions of parameter space where the saddle points exist, but leads to the complicated task of finding roots of polynomials of high order. On the other hand, we can use the fact that, at the birth of the cycle, solutions are confined to invariant lines. The flow on these lines cannot be obstructed by other equilibrium points, unless they are part of the cycles. This leads to the following conditions for existence of a cyclic solution:

$$-x+\tanh[c(x-\lambda+\epsilon)]>0, \tag{3}$$

$$-x+\tanh[c(x+\lambda+\epsilon)]<0. \tag{4}$$

When $\epsilon=0$, the left-hand sides of Eqs. (3) and (4) each have a local minimum and a local maximum for $x\in(-1:1)$. When $\epsilon>0$, both extrema are shifted vertically. Thus, Eq. (3) is satisfied for $\epsilon=0$ as well as $\epsilon>0$. Hence, we only have to worry about condition (4). To find the critical point λ_c, we then compute the local maximum of Eq. (4), set it to zero, and solve for λ. We get

$$\lambda_c=-\epsilon+\frac{1}{c}\ln(\sqrt{c}+\sqrt{c-1})-\tanh[\ln(\sqrt{c}+\sqrt{c-1})]. \tag{5}$$

To verify this result, we conducted, numerically, a two-parameter continuation analysis using AUTO with $c=3$, see Fig. 3. The dark diagonal line represents the loci of the heteroclinic cycle obtained numerically by AUTO, which shows very good agreement with the analytic loci determined by Eq. (5) (superimposed square points). The other curves represent the loci of HB points, which in all cases lead to unstable periodic solutions. The oscillation frequency ω, as a function of the system parameters, can be calculated from its period T. Near the cycle, T is essentially the time required to travel along the invariant lines. By symmetry, the time spent on each branch is approximately the same. Hence, $T\approx 6\int_{-1}^{1}dt$, where $dt\approx dx/(-x+\tanh[c(x-\lambda+\epsilon)])$, and the integral must be evaluated numerically. In Fig. 4, we examine the relation between frequency and system parameters λ and ϵ with $c=3$. The zero-frequency line in the $(\lambda,\ \epsilon)$ plane is in very good agreement with our expression (5) for the critical coupling strength. Then a numerical approximation for the frequency dependence on the system parameters can be obtained:

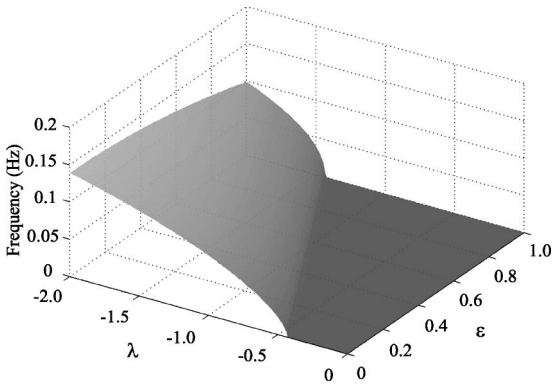

FIG. 4. Frequency response vs system parameters λ and ϵ, for coupled system (2) with $N=3$ and $c=3$.

$$\omega=0.115\sqrt{-\lambda-0.85\epsilon-0.4345}. \tag{6}$$

As mentioned earlier, the oscillations are not sinusoidal, however, they tend to being sinusoidal for large coupling strength magnitude ($\lambda\ll\lambda_c$; recall that $\lambda_c<0$). It is instructive to note that there is a precise $2\pi/3$ phase difference between solutions, which suggests that the limit cycle oscillations form a traveling wave pattern created via a global bifurcation of a heteroclinic cycle. The amplitudes of the individual oscillations are (for any λ and $\epsilon=0$) ± 1, corresponding to the locations of the stable minima of the potential $U(x)$ for each individual uncoupled element with $\epsilon=0$; with increasing ϵ, one observes a displacement in the wave forms of Fig. 5. One may also compute the summed output $X(t)=\Sigma_i x_i(t)$ which is also shown in Fig. 5. $X(t)$ is almost sinusoidal, and it has frequency 3ω (in general we would expect the summed output to have a frequency $N\omega$). Increasing N decreases the individual oscillation frequency ω; effectively, the onset of the oscillations is delayed, as already observed in a coupled system of two-dimensional elements undergoing a saddle-node bifurcation [9]. Numerical simulations show that ω is very sensitive to small

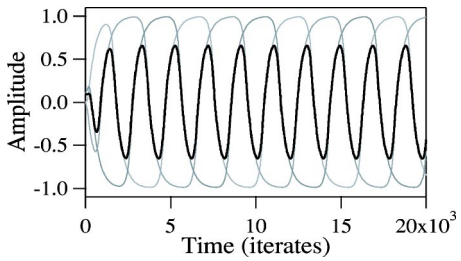

FIG. 5. Time series plot of individual wave forms x_1, x_2 and x_3 (light lines) and their sum (dark line) for $c=3$, $\lambda=-0.650$, $\epsilon=0$.

changes in the target signal strength ϵ; in addition, the mean value of the oscillation amplitude is nonzero for finite ϵ. Both these effects can be used to quantify a very weak ''target'' signal ϵ. A very small power source should suffice, in practice, to generate and sustain the oscillations once the sensor is activated. This is significant for practical applications. For example, the recently proposed dynamical fluxgate magnetometer [4] follows dynamics of form (1), and is typically read out by generating a suprathreshold periodic oscillation via an *external* signal generator. These oscillations lead to identical residence times in the saturation states of the ferromagnetic core, with the target signal breaking this symmetry, and thereby permitting its quantification via the difference in residence times. The summed response $X(t)$ has been observed to be particularly sensitive to the presence of target signal. Simulations show that the mean amplitude of $X(t)$ can be an order of magnitude or more in excess of the corresponding response of a single uncoupled element, externally driven to generate oscillations similar to those shown in Fig. 5. Hence, generating the on-board oscillations via the procedure of this paper holds out the promise of significantly lower on-board power and, potentially, a significant sensitivity enhancement.

In the presence of a noise floor in each element, one would expect not to observe a significant change (introduced solely by the noise) in the frequency ω, as long as the noise strength is much smaller than the energy barrier height in the absence of coupling, noting that the generated oscillations are suprathreshold. The noise floor also guarantees nonidentical initial conditions in the elements of the array; as mentioned above, this is necessary for the oscillatory behavior to exist. The target signal may be quantified via the change in oscillation frequency as well as through a computation of the mean values $\langle x_i(t)\rangle$ or $\langle X(t)\rangle$, or even through spectral or level-crossing techniques.

In conclusion, we must reiterate that the oscillatory behavior observed in the array does *not* occur in a single unforced element. Even when coupled, the number of elements, initial conditions, and the type of coupling are critical conditions for the emergence of this behavior. Hence, the ideas of this paper, while being interesting in their own right, also reveal potential ways to enhance the utility and sensitivity of a large class of nonlinear dynamic sensors (e.g. the magnetometer discussed in Ref. [4], ferroelectric detectors for electric fields, or piezoelectric detectors for acoustics applications) by careful coupling and configuration. A detailed analysis of dynamics (2) in the presence of noise will be the subject of a forthcoming paper.

The authors wish to acknowledge the support from the SPAWAR internal funding (ILIR) program and the Office of Naval Research (Code 331).

[1] V. In *et al.* (unpublished).

[2] M. Golubitsky, I.N. Stewart, and D.G. Schaeffer, *Singularities and Groups in Bifurcation Theory*, Applied Mathematical Science, Vol. II (Springer-Verlag, New York, 1988); D.G. Aronson, M. Golubitsky, and M. Krupa, Nonlinearity **4**, 861 (1991); M. Golubitsky and I. Stewart, *Symmetry and Pattern Formation in Coupled Cell Networks* (Springer-Verlag, New York 1999).

[3] See, e.g., H. Stanley, *Introduction to Phase Transitions and Critical Phenomena* (Oxford University Press, Oxford, 1971).

[4] A.R. Bulsara *et al.*, Phys. Rev. E **67**, 016120 (2003); B. Ando, S. Baglio, A.R. Bulsara, and L. Gammaitoni (unpublished).

[5] L. Gammaitoni and A.R. Bulsara, Phys. Rev. Lett. **88**, 230601 (2002); A. Nikhitin, N. Stocks, and A.R. Bulsara, Phys. Rev. E **68**, 016103 (2003).

[6] E. Doedel and X. Wang, Applied Mathematics Report, California Institute of Technology, 1994 (unpublished).

[7] B. Dionne, M. Golubitsky, and I. Stewart, Nonlinearity **9**, 559 (1996).

[8] M. Krupa, J. Nonlinear Sci. **7**, 129 (1997); P.-L. Buono, M. Golubitsky, and A. Palacios, Physica D **143**, 74 (2000).

[9] J. Acebron, W-J. Rappel, and A.R. Bulsara, Phys. Rev. E **67**, 016210 (2003).